CHEMICAL COMPOSITION AND SOURCE APPORTIONMENT OF $PM_{2.5}$ AT A SUBURBAN SITE IN THE NORTHWESTERN PART OF TURKEY

by

Hatice KARADENIZ[a*], Eda SAGIRLI[b], and Serpil YENISOY-KARAKAS[b]

[a]Scientific, Industrial and Technological Application and Research Center,
Bolu Abant Izzet Baysal University, Bolu, Turkiye
[b]Department of Chemistry, Faculty of Art and Sciences,
Bolu Abant Izzet Baysal University, Bolu, Turkiye

Original scientific paper
https://doi.org/10.2298/TSCI220227219K

In this study, daily fine particulate matters ($PM_{2.5}$) were sampled between February 22, 2011 and February 22, 2012 in Bolu Abant Izzet Baysal University Campus. 277 $PM_{2.5}$ samples were collected by using a stacked filter unit. The 51 elements (Li, Be, Na, K, Mg, Al, P, S, Ca, Ti, V, Cr, Mn, Fe, Co, Ni, Cu, Zn, Ge, As, Se, Rb, Sr, Y, Mo, Cd, Sn, Sb, Cs, La, Ce, Pr, Nd, Eu, Sm, Gd, Tb, Dy, Ho, Er, Tm, Yb, Lu, Hf, W, Pt, Au, Pb, Bi, Tl, Th, U) were determined using ICP-MS technique. The most frequently observed elements were Ti, V, Cr, Mn, Fe, Ce, and Cd in $PM_{2.5}$. Aluminum, Ca, Na, Fe, K, and Mg were the elements having the largest arithmetic means. The concentrations of elements in the summer seasons were higher than the concentrations of elements in the winter season except for As and Bi. Source apportionment of elements was performed by using positive matrix factorization. Five sources were determined for the samples namely sea salt (Na, K, Mg, Ca), coal combustion (As, Pb, Bi, Tl, Cd, Sb, Se, Mo), wood and coal combustion (K, Rb, Se, Cs, Sb, Pb, Bi, Tl, Fe, Mn, Cd), soil (Ca, Mg, Ti, Fe, Y, La, Ce, Pr, Nd, Sm, Gd, Th), and industrial activity – iron-steel works (Cr, Mo, Fe, Ni, Cu, Mn, Cd, Sb, Ca). The factor of wood and coal combustion showed the same trend in the region for the whole year.

Key words*: $PM_{2.5}$, source apportionment, elements, positive matrix factorization, seasonal variation*

Introduction

Increasing air pollution with technology, rapid industrialization, and modernization cause serious health problems for people living in both developing and developed countries [1]. Researchers and governments are focused on the effects of PM on human health. However, there are also effects on the visibility and natural ecosystems which are the more diverse effects of PM [2]. Particles with an aerodynamic diameter of less than 2.5 μm are called fine particles ($PM_{2.5}$) [3] and this fraction has a special concern due to its impact on human health

*Corresponding author, e-mail: haticekaradeniz@ibu.edu.tr

and the environment [4]. Moreover, these particles have a larger specific surface area, a longer residence time in the air, and are more easily transported [3]. Sources of PM can be both natural and anthropogenic. Manmade sources of PM include combustion in mechanical and industrial processes, vehicle emissions, and tobacco smoke. Natural sources include volcanoes, fires, dust storms, and aerosolized sea salt [5].

Studies about PM are being presented that trace metals influence the toxicity of airborne PM. Toxicologically, metals are redox-active and therefore they can induce or catalyze chemical change and help to produce free radicals such as the hydroxyl radical. Therefore, the solubility and existence of the metal in PM are also important [6].

In air quality plans, identification and quantification of sources that contribute PM is an important step to evaluate scenarios for future emissions and control air quality levels. Source apportionment methodologies aim at understanding the origin of pollution [7]. The most widely used methods in source apportionment are receptor models [8]. Positive matrix factorization (PMF) is one of the most broadly used receptor models [8-11].

This paper reported atmospheric levels of $PM_{2.5}$ and trace elements in daily samples collected between February 22, 2011 and February 22, 2012 in Bolu, Turkey. The temporal characteristics, seasonal variations, and sources of air pollution were evaluated to understand the chemical composition of $PM_{2.5}$. The PMF was used for the source apportionment studies. It is expected that the details of the pollution characteristics and the results of source apportionment of $PM_{2.5}$ can help policymakers to take precautions about the reduction of the pollutants in the Bolu atmosphere.

Experimental

Study area, sampling, and analysis of samples

Bolu is located in the Western Black Sea region in Turkey, between Istanbul and Ankara. These cities are important metropolises and industrialized cities in Turkey. In addition, the city is surrounded by urbanized, industrialized cities like Zonguldak, Karabuk, Eskisehir, Duzce, and. Sakarya. There are two highways (D-100 and TEM) connecting Anatolia to Europe crossing in the city of Bolu. Although it has nine districts and 512 villages, 53% of the total population lives in the city center [12]. The climate of the city is like Black Sea Region and generally is warm in summer, cold in winter, and rainy in all seasons. The climate is also affected by Marmara and central Anatolia [12]. The height of mountains increases from north to south and from west to east around the city center and this causes the air-flow to be trapped in this city. The main wind direction is the WSW direction. The total area of the province is 845800 hectares and 18% of the total area is used for agriculture. Possible major anthropogenic sources in Bolu are domestic heating, industrial and agricultural activities, and traffic [12].

Sampling was performed on the roof of the old presidency building on the campus of Bolu Abant Izzet Baysal University (40° 42.864' N; 31° 31.035' E) which is 12 km far away from the city center. Air currents entered the city center from the sampling point. Therefore, it is an important sampling point to study the long-range transport of pollutants from Europe, Russia, and the cities such as Istanbul, Kocaeli, and Karabuk. Daily $PM_{2.5}$ samples were collected by using a *GENT* stacked filter unit between the 22nd of February 2011 and the 22nd of February 2012. Nuclepore 47 mm polycarbonate filters with pore sizes of 0.4 μm were used for sampling. The device has a PM_{10} pre-impactor and contains two filters, PM_{10} and $PM_{2.5}$. Weather Link meteorology station was used to take meteorological parameters.

The filters were conditioned before and after sampling in a glass cabinet at 25% relative humidity and 25 ℃ located in a clean room. The sampled filters were weighed and prepared for analysis. Sample filters and blank samples were kept in petri dishes in the cold room (+4 ℃) until analysis. Samples were prepared for analysis by microwave acid digestion. One mL supra pure 40% HF (Merck) and 5 mL 65% ultrapure HNO_3 were used for the digestion. After the microwave digestion process, the vessels were cooled to room temperature and poured into open digestion teflon vessels by washing with deionized water (18.1 MΩ Ultrapure Water). Analysis of filters was performed using an Perkin Elmer inductively coupled plasma mass spectrometry (ICP-MS) for a total of 51 elements (Li, Be, Na, K, Mg, Al, P, Ca, Ti, V, Cr, Mn, Fe, Co, Ni, Cu, Zn, Ge, As, Se, Rb, Sr, Y, Mo, Cd, Sn, Sb, Cs, La, Ce, Pr, Nd, Eu, Sm, Gd, Tb, Dy, Ho, Er, Tm, Yb, Lu, Hf, W, Pt, Au, Pb, Bi, Tl, Th, U). The Operating conditions for ICP-MS were shown in Table S1 in *Appendix*.

Quality control/quality assurance

In this study, the calculation of LOD for each element was based on replicate analyses using blank samples and expressed as the concentration value corresponding to three times the standard deviation of ten replicate analyses of a blank filter' were used. The recovery and reproducibility of acid digestion was also evaluated. A certified reference materials, SRM 1648a-Urban PM (NIST), was analyzed to check the accuracy of the analysis method for a quality control. The validation results of the experiment was summarized in Table S2 and Table S3 in *Appendix*.

Source apportionment using PMF model

Source apportionment helps give information about pollution sources and their contributions to air pollution [7]. The PMF model was one of the receptor models developed by the US Environmental Protection Agency (EPA) [13]. This multivariate factor analysis tool uses a matrix of speciated sample data into two matrices. Each data point is interpreted individually and uses sample concentration the sample data uncertainty which is determined by the user [14]. The minimized objective function, Q, in PMF:

$$Q = \sum_{i=1}^{n}\sum_{j=1}^{m}\left[\frac{x_{ij} - \sum_{k=1}^{p} g_{ik} f_{kj}}{u_{ij}}\right] \tag{1}$$

where x is the data matrix of i number of samples by j chemical species that were measured, and u is the uncertainties.

In this study, the mass concentrations of 43 elements determined in fine PM samples in both seasons were included in the PMF analysis. Due to detection in fewer analyzed samples, Tb, Ho, Tm, Lu, Eu, Pt, and Au were not used in the PMF analysis. The equation-based uncertainty file was prepared. The program examines the relationship between concentration and uncertainty values and classifies elements as bad, weak, and strong species. The weak elements were Ca, V, Ni, Cu, Se, Mo, Cd, Sb, Cs, La, Ce, Pb, Bi, and the bad elements were Li, Al, Co, Zn, Ge, Sr, Sn, Dy, Er, Yb, Hf, W, U in our study. The 22 samples were discarded because of not having residuals between +3 and −3. Displacement and bootstrap analysis showed that the results were acceptable. The Q_{robust} and Q_{true} values are 8109.64 and 8741.44, respectively. Error code Bootstrap (BS) error estimation is used to detect and estimate the disproportionate effects of a small set of observations on the solution and the effects of rotational ambiguity on the solution. No error code (0) which means that DISP analysis results

were considered valid [14]. The minimum number of BS runs, 20, was performed and 100% mapping was observed for all factors. Eighty percent mapping of each factor represents that the PMF solution is acceptable [14].

Result and discussion

General characteristics and seasonal variations of data

Statistical summaries for all measured species in $PM_{2.5}$ are shown in tab. 1. The observed high standard deviations were related to variations in the meteorological conditions, physical and chemical transformations, air mass transport patterns, and the variations in emissions between samples. While soil-originated elements Al, Ca, K, Fe, and Mg have the greatest concentrations, the most frequently observed elements were Ti, V, Cr, Mn, Fe, Ce, and Cd in $PM_{2.5}$. The lowest concentrations were seen in Tm, Lu, and Pt. The most frequently observed elements were Ti, V, Cr, Mn, Fe, Ce, and Cd.

Table 1. Summary statistics of elemental concentrations in fine fraction aerosols [ng m^{-3}]

Element	N	Arithmetic mean	Standard deviation	Median	Element	N	Arithmetic mean	Standard deviation	Median
Li	269	0.2	0.4	0.1	Sn	273	1	1	0.5
Be	154	0.01	5×10^{-3}	0.01	Sb	272	1	0.5	1
Na	274	217	275	104	Cs	273	0.1	0.1	0.1
K	272	184	111	163	La	275	0.1	0.2	0.1
Mg	267	73	89	44	Ce	276	0.3	1	0.2
Al	270	1342	3301	218	Pr	270	0.02	0.02	0.01
P	276	8	9	6	Nd	275	0.1	0.1	0.05
Ca	271	756	1035	465	Eu	162	0.01	0.02	5×10^{-3}
Ti	276	11	10	8	Sm	253	0.01	0.01	0.01
V	276	1	1	1	Gd	264	0.01	0.01	0.01
Cr	276	20	21	15	Tb	52	4×10^{-3}	2×10^{-3}	3×10^{-3}
Mn	276	4	3	4	Dy	248	0.01	0.01	0.01
Fe	276	199	646	136	Ho	59	4×10^{-3}	2×10^{-3}	3×10^{-3}
Co	265	2	7	0.1	Er	243	0.1	0.4	0.01
Ni	275	6	14	3	Tm	10	4×10^{-3}	1×10^{-3}	4×10^{-3}
Cu	273	6	8	4	Yb	214	0.01	0.01	4×10^{-3}
Zn	272	27	27	18	Lu	18	3×10^{-3}	1×10^{-3}	3×10^{-3}
Ge	224	0.1	0.1	0.1	Hf	229	0.03	0.04	0.02
As	275	1	1	1	W	268	0.2	0.3	0.1
Se	252	0.4	0.2	0.3	Pb	270	12	29	6
Rb	274	1	0.3	0.5	Bi	255	0.1	0.1	0.05
Sr	272	4	14	2	Tl	254	0.1	0.1	0.04
Y	273	0.05	0.05	0.04	Th	261	0.03	0.04	0.02
Mo	272	0.3	0.3	0.2	U	210	0.1	0.1	0.01
Cd	276	5	35	0.4	$PM_{2.5}$	266	17782	16305	16247

The weather condition of Bolu is similar to Black Sea Region and there is an almost continuous need for a heating process. In summer, the heating process occurs especially at higher altitudes of the Bolu Mountains, not in the city center. Therefore, the sampling period has been divided into two seasons, winter (October-April) and summer (June-September). Winter to summer ratios was calculated by using arithmetic mean values of total elemental

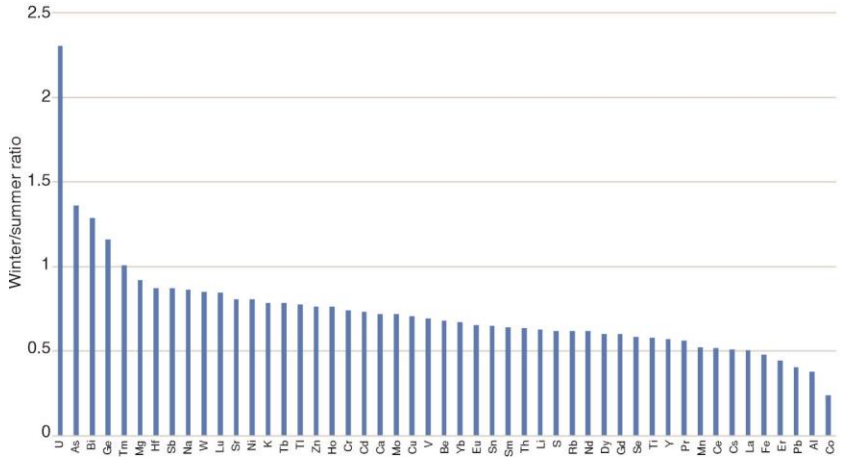

Figure 1. Winter to summer ratio of each element in the sampling period

concentrations and illustrated in fig. 1. Uranium, As and Bi had higher concentrations in winter The arithmetic means of the summer season were lower than the winter season probably due to the coal-burning in winter. The crustal elements like Al, Mn, and Fe are normally in higher concentrations in summer than in winter. There are resuspended PM in air in dry season. However, the concentrations of anthropogenic elements like Co, Pb, Mo, Ni, Se, Sn, and K had higher concentrations in summer than in winter. This may be the result of heavy rain events in winter that scavenge the pollutants.

Source apportionment

Five sources were obtained by the PMF 5.0 model solution with bootstrap and displacement tests. The estimated sources are summarized in tab. 2. The G-score combined wind sector analysis was drawn by using the G-scores and dominant wind sector of each sampling day to investigate the pollution sources of each factor in fig. 2. Furthermore, the identification of factors was evaluated with the tracer elements and sources of elements were given for each factor. Figure 3 displays the relative contribution of each element to each factor.

Table 2. Source profiles of $PM_{2.5}$

Factors	Elements	Explained percentage
Sea salt	Na, K, Mg, Ca	11.5%
Coal combustion	As, Pb, Bi, Tl, Cd, Sb, Se, Mo	12.5%
Wood and coal combustion	K, Rb, Se, Cs, Sb, Pb, Bi, Tl, Fe, Mn, Cd	27.3%
Soil	Ca, Mg, Ti, Fe, Y, La, Ce, Pr, Nd, Sm, Gd, Th	29.7%
Industrial activity (iron-steel works)	Cr, Mo, Fe, Ni, Cu, Mn, Cd, Sb, Ca	19.0%

Factor 1 was explained by 11.5% of total concentration and characterized by the elements Na, K, Mg, and Ca. The Na, Ca, and Mg are very well-known tracers of sea salt [15]. The greatest G-scores were seen on 16th May 2011 and 25th May 2011. When the back trajectories belonging to these days were examined, it was seen that the air currents coming from the Black Sea region were dominant. This factor affects the samples in the spring, summer, and autumn seasons.

Factor 2 had high loadings of As, Pb, Bi, Tl, Cd, Sb, Se, and Mo and was explained by 12.5%. The As, Se, Bi, and Tl are indicator elements of coal combustion [16, 17]. Coal

combustion also may be responsible for Sb and Tl emissions [18]. The effects of this factor on $PM_{2.5}$ are more visible since the winter G-scores were greater. The G-score combined wind sector analysis was evaluated and high scores originated from ENE, W, and SW sectors. These sectors cover most coal-burning heating areas in the city center of Bolu.

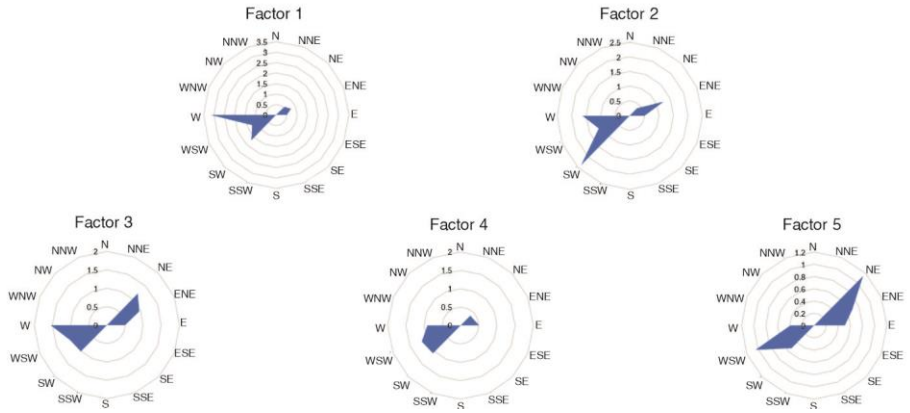

Figure 2. Wind roses for each factor

Factor 3 had high loadings of K, Rb, Se, Cs, Sb, Pb, Bi, Tl, Fe, Mn, and Cd. This factor is identified as coal and wood burning factor owing to the presence of combustion tracers. The As and Se are the marker elements for coal combustion and K and Rb are the marker elements for wood burning [16, 19]. In the villages of the city, wood and coal are used for heating at the same time. The wind sector analysis results also pointed to the W, WSW, NE, and ENE directions where the settlement areas around the sampling point are located, fig. 2. Since wood and coal burning continue throughout the year, the G-score values do not change throughout the year. Especially in the summer season, heating is needed in the evenings due to the low temperatures in the high-altitude villages. The explained part of the factor is 27.3%.

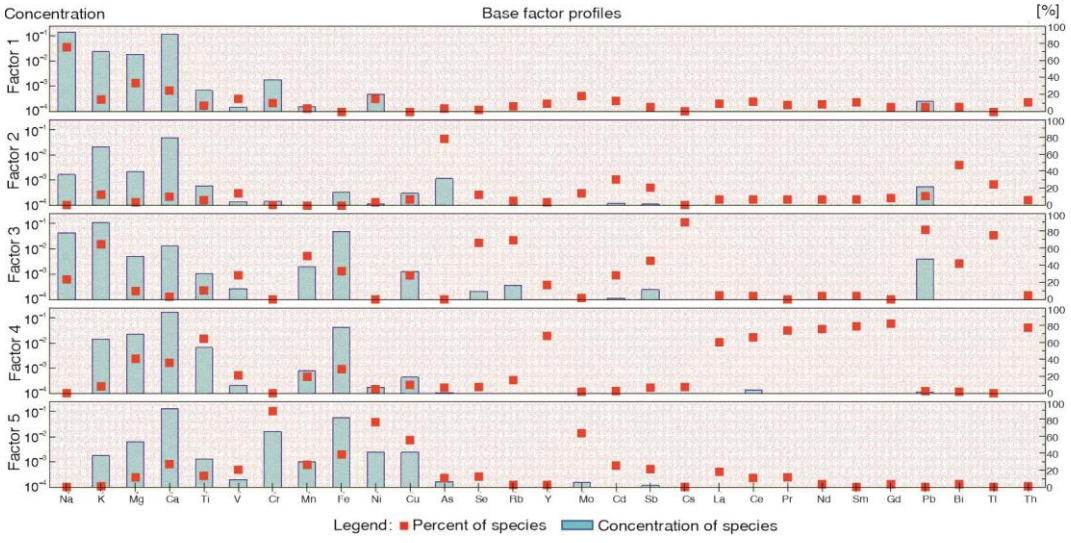

Figure 3. Compositional profiles (species percentage and concentration) corresponding to each factors

Factor 4 was identified as the soil factor, because it included high loadings of crustal elements such as Ca, Mg, Ti, Fe, Y, La, Ce, Pr, Nd, Sm, Gd, and Th. When the days with high G-scores in the PMF analysis for this factor were examined, air-flows coming from North Africa and the Middle East on the 29th of April 2011 and 19th of May 2011 were observed, respectively. The back trajectories of these days can be seen in fig. 4.

The last factor was highly loaded with the elements Cr, Mo, Fe, Ni, Cu, Mn, Cd, Sb, and Ca. Anthropogenic elements such as Cr, Ni, Mn, Fe, and Mo are released from iron-steel works [20]. The back trajectories corresponding to the greatest G-scores of Factor 5 are given in fig. 4. The dominant wind sectors were WSW and NE sectors, fig. 2. Air masses coming from Europe or Russia also pass through Karabük carrying the pollution of Karabük iron-steel factory.

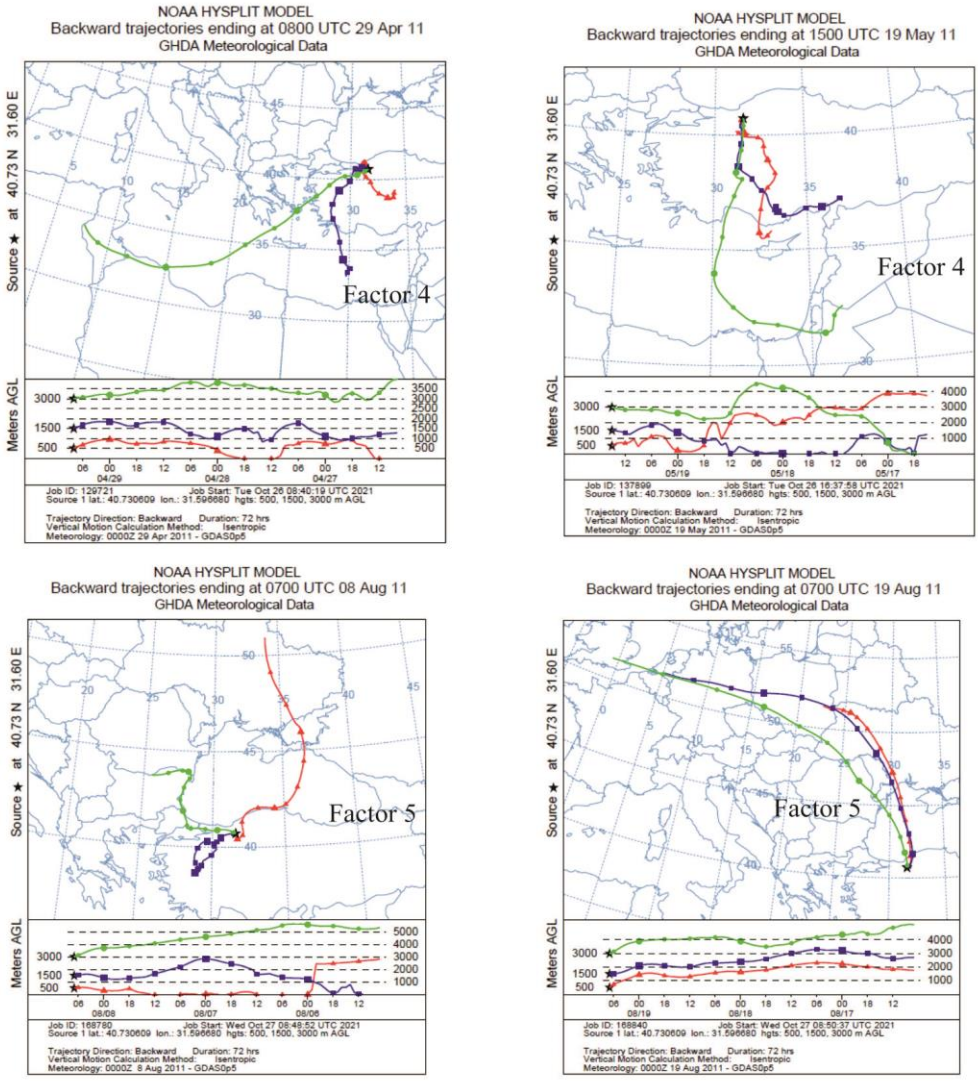

Figure 4. The back trajectories of dates that had greater G-scores for Factor 4 and Factor 5

Conclusion

In this study, daily fine $PM_{2.5}$ was sampled between the 22nd of February 2011 and the 22nd of February 2012 in Bolu Abant Izzet Baysal University Campus (BAIBU), Turkey. The most frequently observed elements were Ti, V, Cr, Mn, Fe, Ce, and Cd in $PM_{2.5}$. The Al, Ca, Na, Fe, K, and Mg were the elements having the greatest arithmetic means. In the Bolu station, the most frequent annual winds were from the WSW sector carrying the long-range pollutants to the sampling station. The concentrations of elements in the summer seasons were higher than the concentrations of elements in the winter season except for As and Bi. Five Factors were identified from PMF. They were sea salt, coal combustion, wood and coal combustion, soil, and industrial activities (iron-steel-works). However, higher G-scores for the coal combustion factor were observed in winter. Long-range transportation is an important pollutant source for the sampling area for the elements.

Acknowledgment

This study was financially supported by TUBITAK (grant number 111Y321).

References

[1] Gupta, P., *et al*., Measurement of PM_{10}, $PM_{2.5}$ and Black Carbon and Assessment of their Health Effects in Agra, A Semiarid Region of India, *Proc. of the Indian Nat. Sci. Acad., 86* (2019), 3, pp. 667-679
[2] Grantz, D. A., *et al*., Ecological Effects of Particulate Matter, *Environment International, 29* (2003), 2-3, pp. 213-239
[3] Javed, W., *et al*., Source Apportionment of Organic Pollutants in Fine and Coarse Atmospheric Particles in Doha, Qatar, *J. Air Waste Manage. Assoc., 69* (2019), 11, pp. 1277-1292
[4] Chalvatzaki, E., *et al*., Characterization of Human Health Risks from Particulate Air Pollution in Selected European Cities, *Atmosphere (Basel)., 10* (2019), 2, pp. 1-16
[5] Anderson, J. O., *et al*., Clearing the Air: A Review of the Effects of Particulate Matter Air Pollution on Human Health, *J. Med. Toxicol., 8* (2012), 2, pp. 166-175
[6] Harrison, R. M., Yin, J., Particulate Matter in the Atmosphere: Which Particle Properties are Important for Its Effects on Health?, *Sci. Total Environ., 249* (2000), 1-3, pp. 85-101
[7] Thunis, P., *et al*., Source Apportionment to Support Air Quality Planning: Strengths and Weaknesses of Existing Approaches, *Environ. Int., 130* (2019), Jan., 104825
[8] Jiang, N., *et al*., Characteristics of Mass Concentration, Chemical Composition, Source Apportionment of $PM_{2.5}$ and PM_{10} and Health Risk Assessment in the Emerging Megacity in China, *Atmos. Pollut. Res., 9* (2018), 2, pp. 309-321
[9] Yenisoy-Karakas, S., *et. al*., Intraday and Interday Variations of 69 Volatile Organic Compounds (BVOC and AVOC) and their Source Profiles at a Semi-Urban Site, *Sci. Total Environ. 723* (2020), June, 138028
[10] Wang, J., *et al*., Contamination Characteristics and Possible Sources of PM_{10} and $PM_{2.5}$ in Different Functional Areas of Shanghai, China, *Atmos. Environ., 68* (2013), 3663, pp. 221-229
[11] Kassomenos, P. A., *et al*., Study of PM_{10} and $PM_{2.5}$ Levels in Three European Cities: Analysis of Intra and Inter Urban Variations, *Atmos. Environ., 87* (2014), Apr., pp. 153-163
[12] ***, Bolu Province Environmental Perspective Report (2010) T.C. Directorate of Environment and Urban Planning, Turkey
[13] Gao, J., *et al*., Seasonal and Spatial Variation of Trace Elements in Multi-Size Airborne Particulate Matters of Beijing, China: Mass Concentration, Enrichment Characteristics, Source Apportionment, *Chem, Speciat. Bioavailab., 99* (2014), Dec., pp. 257-265
[14] ***, US-EPA, EPA Positive Matrix Factorization (PM F)5.0 Fundamentals and, Environ. Prot. Agency Off. Research Dev. Publishing House Washington, DC 20460, 2014, pp. 136
[15] White, W. H., Chemical Markers for Sea Salt in IMPROVE Aerosol Data, *Atmos. Environ., 42* (2008), 2, pp. 261-274
[16] Yenisoy-Karakas, S., Biomonitoring of the Atmospheric Pollutants at Western Anatolia, Ph. D. thesis, METU Graduate School of Natural Applied Science, Ankara, Turkey, 2000

[17] Calvo, A. I., *et al*., Research on Aerosol Sources and Chemical Composition: Past, Current and Emerging Issues, *Atmos. Res., 120-121* (2013), Feb., pp. 1-28
[18] Xu, M., *et al*., Status of Trace Element Emission in a Coal Combustion Process: A Review, *Fuel Process. Technol., 85* (2004), 2-3, pp. 215-237
[19] Frati, L., *et al*., Problems Related to Lichen Transplants to Monitor Trace Element Deposition in Repeated Surveys: A Case Study from Central Italy, *J. Atmos. Chem., 52* (2005), 3, pp. 221-230
[20] Dragović, S., Mihailović, N., Analysis of Mosses and Topsoils for Detecting Sources of Heavy Metal Pollution: Multivariate and Enrichment Factor Analysis, *Envir. Monit. Assess., 157* (2009), 1-4, pp. 383-390

Appendix

Table S1. Operating conditions for the Perkin Elmer-ICP-MS- DRC-e

Parameter	Value
RF power [W]	1100
Plasma gas flow [Lpm]	15
Auxiliary gas flow [Lpm]	1.2
Nebulizer	Gemtip crossflow
Nebulizer gas flow [Lpm]	0.96
Sampling cone (orifice dia., mm)	Platinum (1.1)
Skimmer cone (orifice dia., mm)	Platinum (0.9)
Injector	Alumina
Peristaltic pump flow [rpm]	20
Spray chamber	Ryton Scott
Scanning mode	Both (analog and pulse)
Number of Scans (sweeps/reading) for each isotope	20
Ion lens setting	Adjusted to obtain maximum signal/noise ratio (CeO/Ce < %3, Ba++/Ba < % 3), Background 220: 1.2, Background 8.5: 2.1
Auto sampler	CETAC ADX-500
Rinse time [s]	45
Sampe Uptake time (flush) [s]	35

Table S2. The SRM NIST 1648a Urban PM method accuracy results (number of analyses: 10)

	Results (Average concentration ± STD) [mgkg^{-1}]			UPM Certificate value [mgkg^{-1}] (Average concetration ± expanded uncertainty) (k = 2)			% Error
Al	3.54%	±	0.74%	3.43%	±	0.13%	3.1
As	115.1	±	4.2	115.5	±	3.9	–0.3
Ca	5.56%	±	0.17%	5.84%	±	0.19%	–4.9
Cd	71.9	±	1.9	73.7	±	2.3	–2.4
Ce	46.4	±	1.5	54.6	±	2.2	–15
Co	17.62	±	0.94	17.93	±	0.68	–1.7
Cr	270	±	21	402	±	13	–33
Cu	570	±	18	610	±	70	–6.5
Fe	3.90%	±	0.20%	3.92%	±	0.21%	–0.6
K	1.05%	±	0.10%	1.06%	±	0.05%	–0.8
Mg	0.82%	±	0.09%	0.81%	±	0.01%	0.9
Mn	775	±	33	790	±	44	–1.8
Na	3455	±	905	4240	±	60	–19
Ni	81	±	1.5	81.1	±	6.8	–0.1
Pb	0.62	±	0.006	0.66%	±	0.033	–5.9
Rb	50	±	3.9	51	±	1.5	–1.1
Sb	41.9	±	0.7	45.4	±	1.4	–7.7
Sr	215	±	5	215	±	17	–0.2
Ti	3678	±	235	4021	±	86	–8.5
V	125	±	2	127	±	11	–1.6
Zn	4647	±	107	4800	±	270	–3.2
Cs[a]	3.3	±	0.1	3.4	±	0.2	–4.3
La[a]	32	±	1	39	±	3	–18
Se[a]	28.3	±	2.2	28.4	±	1.1	–0.5
Sm[a]	3.9	±	0.2	4.3	±	0.3	–9.4
W[a]	4.6	±	0.3	4.6	±	0.3	–0.2
Hf[b]	5.1	±	2	5.2			–2.2

Note: [a] reference value, [b] information value

Table S3. Validation table of analyzed elements by ICP-MS

	Reproducibility % RSD	N	Linear range [μgL^{-1}]	R^2	LOD [μgL^{-1}]	LOQ [μgL^{-1}]
Al	21	10	0.01-200	0.9999	1	4
As	4	10	0.01-200	1.0000	0.01	0.04
Ca	3	10	0.01-2000	1.0000	6	19
Cd	3	10	0.01-200	1.0000	0.01	0.03
Ce	3	10	0.01-40	1.0000	0.01	0.04
Co	5	10	0.01-200	1.0000	0.001	0.002
Cr	8	10	0.01-200	1.0000	0.1	0.3
Cu	3	10	0.01-200	1.0000	0.02	0.07
Fe	5	10	0.01-2000	1.0000	0.1	0.4
K	10	10	0.01-2000	1.0000	0.3	1.2
Mg	10	10	0.01-2000	1.0000	0.1	0.5
Mn	4	10	0.01-200	0.9999	0.02	0.06
Na	26	10	0.01-2000	1.0000	1	3
Ni	2	10	0.01-200	1.0000	0.04	0.12
Pb	1	10	0.01-200	1.0000	0.1	0.2
Rb	8	10	0.01-200	1.0000	0.001	0.005
Sb	2	10	0.01-40	1.0000	0.001	0.004
Sr	2	10	0.01-200	1.0000	0.01	0.02
Ti	6	10	0.01-200	1.0000	0.1	0.3
V	1	10	0.01-200	1.0000	0.01	0.05
Zn	2	10	0.01-200	1.0000	0.02	0.07
Cs	3	10	0.01-200	1.0000	0.001	0.002
La	3	10	0.01-40	1.0000	0.002	0.006
Se	8	10	0.01-200	1.0000	0.01	0.03
Sm	6	10	0.01-40	1.0000	0.001	0.004
W	7	10	0.01-200	1.0000	0.02	0.07
Hf	38	10	0.01-40	1.0000	0.01	0.03
Li	–	0.01-2000	1.0000	0.01	0.04	Li
Be	–	0.01-200	1.0000	0.3×10^{-3}	1×10^{-3}	Be
P	–	0.01-200	1.0000	0.1	0.2	P
S	–	0.01-200	1.0000	0.1	0.4	S
Ge	–	0.01-200	1.0000	0.01	0.04	Ge
Y	–	0.01-40	1.0000	0.002	0.006	Y
Mo	–	0.01-200	1.0000	0.01	0.03	Mo
Sn	–	0.01-40	1.0000	0.01	0.02	Sn
Pr	–	0.01-40	1.0000	0.001	0.003	Pr
Nd	–	0.01-40	1.0000	0.002	0.006	Nd
Eu	–	0.01-40	1.0000	0.001	0.002	Eu
Gd	–	0.01-40	1.0000	0.001	0.005	Gd
Dy	–	0.01-200	1.0000	0.001	0.003	Dy
Er	–	0.01-40	1.0000	0.01	0.03	Er
Yb	–	0.01-40	1.0000	0.4×10^{-3}	1×10^{-3}	Yb
Au	–	0.01-1	0.9991	0.2	0.5	Au
Bi	–	0.01-200	1.0000	0.01	0.02	Bi
Tl	–	0.01-200	1.0000	0.001	0.002	Tl
Th	–	0.01-200	1.0000	0.002	0.007	Th
U	–	0.01-200	1.0000	0.002	0.006	U

Note: SRM NIST 1648a Urban PM is used. N: number of analyses

Paper submitted: February 27, 2022
Paper revised: November 14, 2022
Paper accepted: November 22, 2022